Frontiers in Heat and Mass Transfer (FHMT), 9, 21 (2017)
DOI: 10.5098/hmt.9.21

Global Digital Central
ISSN: 2151-8629

Frontiers in Heat and Mass Transfer

Available at www.ThermalFluidsCentral.org

EFFECT OF HALL CURRENT ON MHD NATURAL CONVECTION HEAT AND MASS TRANSFER FLOW OF ROTATING FLUID PAST A VERTICAL PLATE WITH RAMPED WALL TEMPERATURE

Gauri Shanker Seth* Arnab Bhattacharyya and Rajat Tripathi

Department of Applied Mathematics, Indian Institute of Technology (Indian School of Mines), Dhanbad, Jharkhand, 826004, India

ABSTRACT

A study on unsteady MHD natural convection flow of an optically thin, heat radiating, incompressible, viscous, chemically reactive, temperature dependent heat absorbing and electrically conducting fluid past an exponentially accelerated infinite vertical plate having ramped temperature, embedded in a porous medium is carried out, considering the effects of Hall current and rotation. Governing equations are non-dimensionalized and Laplace Transform Technique is used to find the exact solutions for non-dimensional velocity, temperature and concentration fields. The quantities of physical interest i.e. shear stress at the plate, rate of heat and mass transfers at the plate are also derived. Numerical results for the velocity, temperature and species concentration of the fluid are demonstrated with the help of graphs whereas those of shear stress at the plate, rate of heat and mass transfers at the plate are displayed in tables for various flow parameters. It is observed that fluid velocities as well as fluid temperature profiles are slower in case of ramped temperature plate than those of isothermal plate.

Keywords: Hall current, Natural convection, Magnetic field, Radiation, Heat absorption, Chemical reaction.

1. INTRODUCTION

Mutual influences of heat absorption/generation and thermal radiation on magnetohydrodynamic free convection flow are significant for several scientific, engineering and industrial applications viz. high temperature casting, furnace design, thermo-nuclear fusion, solar power technology, missiles, propulsion devices for aircraft, space vehicles and satellites etc. Therefore, it is worthwhile to analyze the fluid flow problems involving combined effects of temperature dependent heat source/sink and thermal radiation. Considering the significance of such study, Chamkha (2000) investigated the effects of heat generation/absorption and thermal radiation on hydromagnetic boundary layer flow near an accelerating porous surface considering the influence of thermal buoyancy force. Makinde (2012) analyzed hydromagnetic mixed convection flow towards a stagnation point on a vertical plate surrounded by a highly saturated porous medium considering the consequences of radiation and internal heat generation. Mixed convection heat dissipative flow past a wedge in a magnetic field with internal heat generation/absorption, thermal radiation and stress work was inspected by Prasad *et al.* (2013). Veeresh *et al.* (2017) studied the Joule heating and thermal diffusion effects on MHD radiative Casson fluid flow past an oscillating vertical porous plate.

Study of magnetohydrodynamic natural convection flow in a rotating frame is of much significance due to its abundant applications in various fields of science and engineering viz. astrophysics, geophysics, oceanology, aeronautics, meteorology, petrochemical engineering etc. This provoked quite a lot of researchers to carry out a capacious volume of research works on unsteady hydromagnetic rotating flow near a vertical plate under various conditions. Mentions may be made of the research works of Singh (1984), Raptis and Singh (1985), Bestman and Adjepong (1988), Mbeledogu and Ogulu (2007).

Further, Hall effects on MHD viscous flows have vital applications in several engineering problems, viz. development of plasma actuator control of hypersonic flows, efficient Hall thrusters in magnetic propulsion, large-scale pulsed MHD generators, nuclear power reactors, Hall current accelerators, Hall effect joysticks to control hydraulic valves etc. Cowling (1957) highlighted the need to incorporate the effects of Hall current in magnetohydrodynamic flows. Since Hall current tends to induce a secondary flow in the flow-field (Sutton and Sherman, 1965), it plays a crucial role in defining the flow-field characteristics. Due to the huge importance of such physical effect, Pop and Watanabe (1994), Aboeldahab and Elbarbary (2001), Seth *et al.* (2013, 2015) and Das *et al.* (2013) investigated the influence of Hall current on hydromagnetic natural convection flow near a vertical plate, considering various aspects of the problem. Reddy (2014) considered Hall effect, thermal radiation and viscous dissipation on MHD convective flow of a viscous, electrically conducting and incompressible fluid past a stretched vertical sheet. Recently, combined effects of radiation, heat absorption and Hall effect on MHD double-diffusive free convective flow past a stretching sheet was discussed by Sreedevi *et al.* (2016).

Chemical reaction is the process by means of which one set of chemical substances are transformed into another. Moreover, the process of chemical reaction takes place between the fluid and a foreign mass. Usually, chemical reactions can be classified into two major categories viz. Heterogeneous and homogeneous chemical reactions. This depends on whether the chemical reactions are occurring at an interface or as a single phase volume reaction. Study of mass transfer flows taking chemical reaction into account has found numerous important applications in several chemical and hydrometallurgical industries such as catalytic chemical reactors, production of glassware and ceramics, food processing, undergoing endothermic or exothermic chemical reaction etc. Chamkha (2003) investigated MHD flow for a uniformly stretched vertical permeable surface in presence of chemical reaction and heat generation/absorption. Afify (2004) discussed the impact of heat radiation on natural convection flow past an isothermal vertical cone surface taking into account the chemical reaction. Other

* Corresponding author. Email: seth.gs.am@ismdhanbad.ac.in

Global Digital Central
ISSN: 2151-8629

interesting results regarding chemical reaction can be found in the research works of Muthucumaraswamy *et al.* (2006), Ibrahim *et al.* (2008), Chamkha *et al.* (2011), Bhattacharya and Layek (2012), Seth *et al.* (2014), Satya Narayana *et al.* (2016), Nagaraju *et al.* (2016) and Hayat *et al.* (2017).

Researchers usually modelled natural convection flows under the conventions of a uniform surface temperature. But in several physical circumstances, the temperature of the bounding surface may necessitate the consideration of non-uniform or arbitrary wall conditions. Moreover, there may occur step discontinuities in the surface temperature. In view of this fact, many researchers explored free convection from a vertical plate with step discontinuities in the surface temperature. Some of the related investigations are due to Hayday *et al.* (1967), Lee and Yovanovich (1991). Also, several researchers investigated unsteady hydromagnetic free convection flow past a vertical plate with ramped wall temperature considering various aspects of the problem. Some of the relevant studies are due to Chandran *et al.* (2005), Rajesh and Chamkha (2014), Kundu *et al.* (2014), Seth and Sarkar (2015) and Seth *et al.* (2016).

The present work intents to examine the influences of rotation and Hall current on transient magnetohydrodynamic free convection flow of a chemically reactive, optically thin heat radiating and heat absorbing fluid past a moving vertical plate in a fluid saturated porous medium considering ramped wall temperature.

2. MATHEMATICAL FORMULATION

Consider an unsteady magnetohydrodynamic free convection flow of an electrically conducting, incompressible, viscous, chemically reactive, optically thin radiating and heat absorbing fluid past an exponentially accelerated moving vertical plate of infinite extent with ramped wall temperature, embedded in a uniform porous medium taking Hall current and rotation into account. Cartesian co-ordinate system (x', y', z') is selected in a fashion where x'-axis is taken along the vertical plate in upward direction, y'-axis is normal to the plate and z'-axis is perpendicular to $x'y'$ plane. The fluid flow is assumed to be under the influence of a uniform magnetic field B_0, acting parallel to y'-axis. Both the fluid and the plate rotate in unison about y'-axis with a uniform angular velocity Ω in anticlockwise direction. Initially i.e. at time $t' \le 0$, both the plate and the fluid are kept at rest with uniform temperature T'_∞ and the concentration of the species at the surface of the plate as well as at every point within the fluid is kept at a uniform concentration C'_∞. At time $t' > 0$, plate is exponentially accelerated with velocity $U_0 e^{a't'}$ in x'-direction (U_0 being characteristic velocity). The temperature of the plate is raised or lowered to $T'_\infty + (T'_w - T'_\infty)t'/t_0$ when $0 < t' < t_0$ and is maintained at uniform temperature T'_w thereafter i.e. when $t' > t_0$. Also, at time $t' > 0$, the species concentration is elevated to a uniform species concentration C'_w and is maintained thereafter. It is presumed that a uniform chemical reaction of order one ensues with a constant rate K'_r between the fluid and dispersing species.

The geometry of the physical problem is presented in Figure 1. Fluid is metallic liquid or partially ionized, having a very small magnetic Reynolds number. Hence, the magnetic field induced due to the fluid flow is insignificant in comparison to the applied one (Cramer and Pai, 1973). Thus, the magnetic field becomes $\vec{B} = (0, B_0, 0)$. Since, the plate is infinite in x' and z' directions, all physical parameters excluding pressure are dependent on y' and t'.

In light of above assumptions, the equations presiding the unsteady MHD free convection flow of an optically thin heat radiating, incompressible, viscous, chemically reactive, temperature dependent heat absorbing/generating and electrically conducting fluid past an exponentially accelerated infinite vertical plate having ramped temperature, in a porous medium, considering the effects of Hall current and rotation, under the approximation proposed by Boussinesq, are specified as:

$$\frac{\partial u'}{\partial t'} + 2\Omega w' = \nu \frac{\partial^2 u'}{\partial y'^2} - \left(\frac{\sigma B_0^2}{\rho}\right)\frac{u' + m w'}{1 + m^2} - \nu \frac{u'}{K'_1} + g\beta'(T' - T'_\infty) + g\beta^*(C' - C'_\infty), \tag{1}$$

$$\frac{\partial w'}{\partial t'} - 2\Omega u' = \nu \frac{\partial^2 w'}{\partial y'^2} + \left(\frac{\sigma B_0^2}{\rho}\right)\frac{m u' - w'}{1 + m^2} - \nu \frac{w'}{K'_1}, \tag{2}$$

$$\frac{\partial T'}{\partial t'} = \frac{k}{\rho c_p}\frac{\partial^2 T'}{\partial y'^2} - \frac{1}{\rho c_p}\frac{\partial q'_r}{\partial y'} - \frac{Q_0}{\rho c_p}(T' - T'_\infty), \tag{3}$$

$$\frac{\partial C'}{\partial t'} = D_m \frac{\partial^2 C'}{\partial y'^2} - K'_r (C' - C'_\infty), \tag{4}$$

where u' - velocity of the fluid along x' - axis, w' - velocity of the fluid along z' - axis, g - gravitational acceleration, ν - kinematic coefficient of viscosity, β' - thermal expansion coefficient, β^* - coefficient of volumetric expansion, T' - temperature of the fluid, C' - concentration of the species, ρ - density of the fluid, σ -electrical conductivity, K'_1 - permeability of porous medium, $m = \omega_e \tau_e$ - Hall current parameter, ω_e - cyclotron frequency, τ_e - electron collision time, k - thermal conductivity of the fluid, c_p - specific heat at constant pressure, D_m - molecular mass diffusivity, K'_r - chemical reaction coefficient, Q_0 - coefficient of heat absorption and q'_r - radiative heat flux.

Initial and boundary conditions for the present investigation are given as

$$u' = 0, w' = 0, T' = T'_\infty, C' = C'_\infty \quad \text{for } y' > 0 \text{ and } t' \le 0, \tag{5a}$$

$$u' = U_0 e^{a't'}, w' = 0, C' = C'_w \quad \text{at } y' = 0 \text{ for } t' > 0, \tag{5b}$$

$$T' = \begin{cases} T'_\infty + (T'_w - T'_\infty)t'/t_0 & \text{at } y' = 0 \text{ for } 0 < t' \le t_0, \\ T'_w & \text{at } y' = 0 \text{ for } t' > t_0, \end{cases} \tag{5c}$$

$$u' \to 0, w' \to 0, T' \to T'_\infty, C' \to C'_\infty \quad \text{as } y' \to \infty \text{ for } t' > 0. \tag{5d}$$

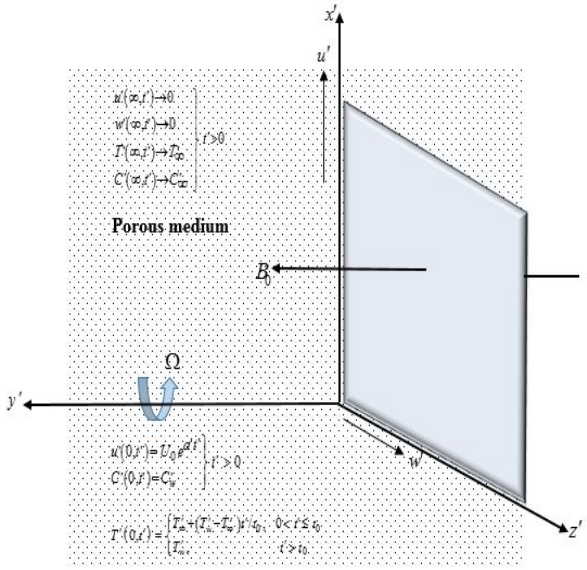

Fig. 1 Schematic diagram of the physical problem

Global Digital Central
ISSN: 2151-8629

Local radiant absorption for an optically thin grey fluid is presented as (Raptis, 2011)

$$\frac{\partial q_r'}{\partial y'} = -4a^*\sigma^*\left(T_\infty'^4 - T'^4\right), \tag{6}$$

where a^* denotes the coefficient of heat absorption and σ^* represents Stefan-Boltzmann constant.

Assuming that the temperature difference within the fluid in the boundary layer region and the free stream is small enough, so that we can express T'^4 as a linear function of T' by Taylor series expansion of T'^4 about T_∞'. Thus, ignoring the second and higher order terms, we have

$$T'^4 = 4T_\infty'^3 T' - 3T_\infty'^4. \tag{7}$$

Making use of Eqs. (6) and (7), equation (3) becomes

$$\frac{\partial T'}{\partial t'} = \frac{k}{\rho c_p}\frac{\partial^2 T'}{\partial y'^2} - \frac{Q_0}{\rho c_p}\left(T' - T_\infty'\right) - \frac{16a^*\sigma^* T_\infty'^3}{\rho c_p}\left(T' - T_\infty'\right). \tag{8}$$

To represent Eqs. (1), (2), (4) and (8) in dimensionless form, following non-dimensional variables and parameters have been introduced:

$$\left.\begin{aligned}
&y = \frac{y'}{U_0 t_0},\ t = \frac{t'}{t_0},\ u = \frac{u'}{U_0},\ w = \frac{w'}{U_0},\ K^2 = \frac{\Omega\nu}{U_0^2},\ a = a'\frac{\nu}{U_0^2},\ M^2 = \frac{\sigma B_0^2\nu}{\rho U_0^2},\\
&T = \frac{T' - T_\infty'}{T_w' - T_\infty'},\ C = \frac{C' - C_\infty'}{C_w' - C_\infty'},\ G_r = \frac{\nu g\beta'\left(T_w' - T_\infty'\right)}{U_0^3},\ G_c = \frac{\nu g\beta^*\left(C_w' - C_\infty'\right)}{U_0^3},\\
&K_r = \frac{\nu K_r'}{U_0^2}, K_1 = K_1'\frac{U_0^2}{\nu^2},\ N = \frac{16a^*\sigma^*\nu T_\infty'^3}{U_0^2\rho c_p},\ \phi = \frac{Q_0\nu}{U_0^2\rho c_p},\\
&P_r = \frac{\nu\rho c_p}{k},\ S_c = \frac{\nu}{D_m} \text{ and } t_0 = \frac{\nu}{U_0^2}
\end{aligned}\right\} \tag{9}$$

where $u, w, K^2, a, M^2, G_r, G_c, K_r, K_1, N, \phi, S_c$ and P_r are, respectively, primary fluid velocity, secondary fluid velocity, rotation parameter, surface acceleration parameter, magnetic parameter, thermal Grashof number, solutal Grashof number, chemical reaction parameter, permeability parameter, radiation parameter, heat absorption parameter, Soret number and Prandtl number.

Using (9), Eqs. (1), (2), (4) and (8), are transformed into following non-dimensional form:

$$\frac{\partial u}{\partial t} + 2K^2 w = \frac{\partial^2 u}{\partial y^2} - \frac{M^2}{1+m^2}\left(u + mw\right) - \frac{u}{K_1} + G_r T + G_c C, \tag{10}$$

$$\frac{\partial w}{\partial t} - 2K^2 u = \frac{\partial^2 w}{\partial y^2} + \frac{M^2}{1+m^2}\left(mu - w\right) - \frac{w}{K_1}, \tag{11}$$

$$\frac{\partial T}{\partial t} = \frac{1}{P_r}\frac{\partial^2 T}{\partial y^2} - \left(N + \phi\right)T, \tag{12}$$

$$\frac{\partial C}{\partial t} = \frac{1}{S_c}\frac{\partial^2 C}{\partial y^2} - K_r C, \tag{13}$$

Initial and boundary conditions (5a) to (5d) in dimensionless system, are presented as:

$$u = 0,\ w = 0,\ T = 0,\ C = 0 \quad \text{for} \quad y \geq 0 \text{ and } t \leq 0, \tag{14a}$$

$$u = e^{at}, w = 0, C = 0 \quad \text{at} \quad y = 0 \text{ for } t > 0, \tag{14b}$$

$$T = \begin{cases} t & \text{at } y = 0 \text{ for } 0 < t \leq 1, \\ 1 & \text{at } y = 0 \text{ for } t > 1, \end{cases} \tag{14c}$$

$$u \to 0,\ w \to 0,\ T \to 0,\ C \to 0 \quad \text{as as } y \to \infty,\ t > 0. \tag{14d}$$

Equations (10) and (11) in compact form is given by

$$\frac{\partial F}{\partial t} + \left\{\frac{M^2}{1+im} + \frac{1}{K_1} - 2iK^2\right\}F = \frac{\partial^2 F}{\partial y^2} + G_r T + G_c C, \tag{15}$$

where $F(y,t) = u(y,t) + iw(y,t)$.

Initial and boundary conditions (14a) to (14d), are transformed into

$$F = 0,\ T = 0,\ C = 0 \quad \text{for } y \geq 0 \text{ and } t \leq 0, \tag{16a}$$

$$F = e^{at}, C = 1 \quad \text{at } y = 0 \text{ for } t > 0, \tag{16b}$$

$$T = \begin{cases} t & \text{at } y = 0 \text{ for } 0 < t \leq 1, \\ 1 & \text{at } y = 0 \text{ for } t > 1, \end{cases} \tag{16c}$$

$$F \to 0,\ T \to 0,\ C \to 0 \quad \text{as } y \to \infty,\ t > 0. \tag{16d}$$

3. SOLUTION OF THE PROBLEM

Laplace Transform Technique is used to solve the Eqs. (12), (13) and (15) along with the conditions (16a) to (16d) to obtain the expressions for fluid temperature $T(y,t)$, species concentration $C(y,t)$ and fluid velocity $F(y,t)$, which are presented as:

$$T(y,t) = P(y,t) - H(t-1)P(y,t-1), \tag{17}$$

$$C(y,t) = g_1(y,t,S_c,K_r,0), \tag{18}$$

$$\begin{aligned} F(y,t) = {} & e^{at}g_1(y,t,1,\beta,a) - \frac{a_2}{b_2}[e^{b_2 t}\left\{g_1(y,t,1,\beta,b_2) - g_1(y,t,S_c,K_r,b_2)\right\} \\ & -\left\{g_1(y,t,1,\beta,0) - g_1(y,t,S_c,K_r,0)\right\}] - \\ & a_1\left[G(y,t) - H(t-1)G(y,t-1)\right], \end{aligned} \tag{19}$$

where

$$\begin{aligned} G(y,t) = {} & \frac{1}{b_1^2}[e^{b_1 t}\left\{g_1(y,t,1,\beta,b_1) - g_1(y,t,P_r,N+\phi,b_1)\right\} - \\ & \left\{g_1(y,t,1,\beta,0) - g_1(y,t,P_r,N+\phi,0)\right\} - \\ & b_1\left\{g_2(y,t,1,\beta) - g_2(y,t,P_r,N+\phi)\right\}], \end{aligned}$$

$$P(y,t) = g_2(y,t,P_r,N+\phi),$$

$$a_1 = \frac{G_r}{1-P_r}, \quad a_2 = \frac{G_c}{1-S_c}, \quad b_1 = \frac{P_r(N+\phi)-\beta}{1-P_r}, \quad b_2 = \frac{S_c K_r - \beta}{1-S_c} \quad \text{and}$$

$$\beta = \frac{M^2}{1+im} + \frac{1}{K_1} - 2iK^2.$$

$H(t-1)$ represents Heaviside unit step function.

The expressions for g_1 and g_2 are provided in Appendix.

3.1 Solutions for unit Prandtl number (P_r) and unit Schmidt number (S_c)

We can see that the analytical solution (19) representing fluid velocity $F(y,t)$ is not valid when we consider $P_r = 1$ and $S_c = 1$. Since Prandtl number is a non-dimensional parameter representing the ratio of diffusion of momentum to the diffusion of heat in a fluid and Schmidt number is a non-dimensional parameter representing the ratio of diffusion of momentum to diffusion of mass in a fluid therefore, the particular cases $P_r = 1$ and $S_c = 1$ correspond to the fluids having same order of magnitude of viscous, thermal and concentration boundary layer thicknesses. There exist some fluids of practical importance belonging to this category (Chen, 2004). Keeping $P_r = 1$ and $S_c = 1$ in equations (12) and (13) and proceeding through the similar method as earlier, we obtain expressions for fluid velocity, fluid temperature and species concentration in following simplified form:

$$\begin{aligned} F(y,t) = {} & e^{at}g_1(y,t,1,\beta,a) + \gamma_1\left[g_1(y,t,1,\beta,0) - g_1(y,t,1,K_r,0)\right] + \\ & G_1(y,t) - H(t-1)G_1(y,t-1), \end{aligned} \tag{20}$$

$$T(y,t) = P_1(y,t) - H(t-1)P_1(y,t-1), \tag{21}$$

$$C(y,t) = g_1(y,t,1,K_r,0), \tag{22}$$

where

$$G_1(y,t) = \gamma_2\left[g_2(y,t,1,\beta) - g_2(y,t,1,N+\phi)\right],$$

$$P_1(y,t) = g_2(y,t,1,N+\phi), \quad \gamma_1 = \frac{G_c}{K_r - \beta} \text{ and } \gamma_2 = \frac{G_r}{(N+\phi)-\beta}.$$

3.2 Solutions for isothermal plate

Expressions (17) to (19) characterize the exact solutions for the temperature, species concentration and velocity of the fluid when the plate admits the ramped wall condition. To emphasize the effect of rampedness in the temperature of the fluid, it is worthwhile to compare such flows with the one near an exponentially accelerated moving vertical plate with uniform temperature. Accordingly, the solutions for fluid velocity and fluid temperature take the following form:

$$F(y,t) = e^{at} g_1(y,t,1,\beta,a) + \left(\frac{a_1}{b_1} + \frac{a_2}{b_2}\right) g_1(y,t,1,\beta,0) +$$

$$\frac{a_1}{b_1}[e^{b_1 t}\left\{g_1(y,t,P_r,N+\phi,b_1) - g_1(y,t,1,\beta,b_1)\right\} -$$

$$g_1(y,t,P_r,N+\phi,0)] + \frac{a_2}{b_2}[e^{b_2 t}\{g_1(y,t,S_c,K_r,b_2) -$$

$$g_1(y,t,1,\beta,b_2)\} - g_1(y,t,S_c,K_r,0)], \tag{23}$$

$$T(y,t) = g_1(y,t,P_r,N+\phi,0). \tag{24}$$

3.3 Shear stress at the plate

The expressions for primary shear stress τ_x and secondary shear stress τ_z at the plate are given by:

For ramped temperature plate:

$$\tau_x + i\tau_z = \left.\frac{\partial F}{\partial y}\right|_{y=0}$$

$$= e^{at} g_3(t,1,\beta,a) - \frac{a_2}{b_2}[e^{b_2 t}\left\{g_3(t,1,\beta,b_2) - g_3(t,S_c,K_r,b_2)\right\} -$$

$$\left\{g_3(t,1,\beta,0) - g_3(t,S_c,K_r,0)\right\}] -$$

$$a_1\left[G_2(0,t) - H(t-1)G_2(0,t-1)\right], \tag{25}$$

where

$$G_2(0,t) = \frac{1}{b_1^2}[e^{b_1 t}\left\{g_3(t,1,\beta,b_1) - g_3(t,P_r,N+\phi,b_1)\right\} -$$

$$\left\{g_3(t,1,\beta,0) - g_3(t,P_r,N+\phi,0)\right\} - b_1\left\{g_4(t,1,\beta) - g_4(t,P_r,N+\phi)\right\}].$$

For isothermal plate:

$$\tau_x + i\tau_z = \left.\frac{\partial F}{\partial y}\right|_{y=0}$$

$$= e^{at} g_3(t,1,\beta,a) + \left(\frac{a_1}{b_1} + \frac{a_2}{b_2}\right) g_3(t,1,\beta,0) +$$

$$\frac{a_1}{b_1}\left[e^{b_1 t}\left\{g_3(t,P_r,N+\phi,b_1) - g_3(t,1,\beta,b_1)\right\} - g_3(t,P_r,N+\phi,0)\right] +$$

$$\frac{a_2}{b_2}\left[e^{b_2 t}\left\{g_3(t,S_c,K_r,b_2) - g_3(t,1,\beta,b_2)\right\} - g_3(t,S_c,K_r,0)\right]. \tag{26}$$

The expressions for g_3 and g_4 are provided in Appendix.

3.4 Rate of heat transfer at the plate

Expressions for heat transfer rate at the plate which is denoted as N_u (Nusselt number), are presented as:

For ramped temperature plate:

$$N_u = \left.\frac{\partial T}{\partial y}\right|_{y=0} = P_2(0,t) - H(t-1)P_2(0,t-1), \tag{27}$$

where

$$P_2(0,t) = g_4(t,P_r,N+\phi).$$

For isothermal plate:

$$N_u = \left.\frac{\partial T}{\partial y}\right|_{y=0} = g_3(t,P_r,N+\phi,0). \tag{28}$$

3.5 Rate of mass transfer at the plate

Expression for mass transfer rate at the plate, denoted as S_h (Sherwood number), is given as follows:

$$S_h = \left.\frac{\partial C}{\partial y}\right|_{y=0} = g_3(t,S_c,K_r,0). \tag{29}$$

4. RESULTS AND DISCUSSION

Extensive numerical calculations have been carried out to analyse the distributions of fluid velocity, fluid temperature and species concentration in the boundary layer together with shear stresses at the plate, heat and mass transfer rates for both isothermal and ramped temperature plates, to get insight into the physics of the flow regime for several values of flow parameters which characterize the features of the flow. Numerical findings are well demonstrated in Figs. 2 to 26 along with the Tables 1 to 4. Throughout the present investigation, we have chosen fixed values of P_r and S_c as 0.71 (ionized air) and 0.6 respectively.

Figures 2 to 21 portray the behavior of primary and secondary velocities u and w under the effects of the flow parameters $m, M^2, K^2, K_1, G_r, G_c, N, \phi, t$ and a, respectively, in the momentum boundary layer. Figures 2 to 21 clarify that secondary velocity w achieves its maximum near the plate and then starts to decreases gradually for further values of the variable *y*. Impact of Hall current on fluid velocity is illustrated in Figs. 2 and 3. From Figs. 2 and 3 it is detected that, both u and w are getting amplified on increasing m and also the fluid velocity changes more rapidly in case of secondary flow than those of primary flow. This phenomenon is in excellent agreement with the fact that a current, known as Hall current, comes into play in case of an electrically conducting fluid whose density is low and the applied magnetic field is strong. This induced current flows in a direction which is perpendicular to both magnetic and electric fields. Thus, it is a tendency of Hall current to accelerate both the primary and secondary fluid velocities. Figures 4 and 5 reveal that, u is getting decreased on increasing M^2 whereas w rises near the plate and then gradually falls in the region far from the plate. Since, in an electrically conducting fluid, existence of magnetic field tend to induce a retarding body force, referred to as Lorentz force and direction of this force is perpendicular to both the fields. Since M^2 suggests the ratio of electromagnetic body force to viscous force, higher value of M^2 leads to a stronger hydromagnetic body force which tend to decelerate the fluid flow. Therefore, application of external magnetic field is a prevailing tool for hindering the fluid motion. Figures 6 and 7 exhibit the consequence of rotation on the flow-field. From Figs. 6 and 7, it is perceived that, on increasing K^2, u gets decelerated whilst a reverse

Global Digital Central
ISSN: 2151-8629

pattern is noted for w. This is justified with the fact that, rotation induces a force viz. Coriolis force which has a tendency to suppress the primary flow in order to induce the flow in secondary direction. It is inferred from Figs. 8 and 9 that, both u and w get enhanced on increasing K_1. This suggests that, permeability parameter intensifies the fluid flow in both the flow directions. The possible reason behind such behavior of fluid flow is that an increment in the permeability reduces the resistance of the porosity of the medium. As a result of which fluid velocity is getting enhanced. The influences of thermal and solutal buoyancy forces on the primary and secondary fluid velocities have been portrayed in Figs. 10 to 13. Here from these figures we notice that, both primary and secondary fluid velocities increase with the increase of G_r and G_c. Since G_r and G_c measure the relative strengths of thermal and solutal buoyancy forces to viscous force respectively, increasing values of G_r and G_c leads to an increase in thermal and solutal buoyancy forces respectively. Since, fluid flow in this problem is induced due to free convection arising as a result of thermal and solutal buoyancy forces, therefore, these forces will obviously result in speeding up of fluid velocities. Figures 14 to 17 portray the influences of thermal radiation and heat absorption on both primary and secondary fluid velocities. From Figs. 14 to 17 a significant fall in the values of u and w can be observed for increasing values of N and ϕ. In other words, the primary and secondary velocities for highly radiating and heat absorbing fluids are smaller as compared to those of lesser radiating and heat absorbing fluids which is justified because fluid temperature is getting reduced on increasing N and ϕ. Likewise, from Figs. 18 and 19, it is inferred that time t tends to increase the fluid velocities. Further, it is established from Figs. 20 and 21, an increment in the fluid velocities in the region adjacent to the plate as we increase the surface acceleration parameter a and the impact of a gradually becomes negligible in the region far from the plate. This observation proposes that higher plate velocity results in faster fluid motion adjacent to the moving plate.

Figures 22 to 24 have been plotted to investigate the behavior of the temperature of the fluid T for variations in thermal radiation N, heat absorption ϕ and time t within the thermal boundary layer, obtained from Eqs. (17) and (24) for both ramped temperature and isothermal plates. One can perceive that, increased values of N or ϕ cause a significant fall in the fluid temperature T whereas the impact of time is contradictory to that of N or ϕ. Thus, we conclude that thermal radiation and heat absorption lower the fluid temperature whereas with the progress of time the temperature of the fluid rises.

Variations in chemical reaction and time on the concentration field, as calculated from Eq. (18), are elucidated in Figs. 25 and 26. Figure 25 is plotted for both positive and negative values of K_r. It is perceived from Fig. 25 that, a rise in the positive values of K_r causes C to fall significantly. Alternatively, amplifying the negative values of K_r results in an enhancement in C. Since, positive values of K_r corresponds to a destructive kind of chemical reaction and negative values of K_r indicates a chemical reaction of generative kind, thus an improvement in the positive values of K_r implies that the depletion of species is taking place with a healthier rate which in consequence lowers the concentration boundary layer thickness. On the contrary, an enhancement in the negative values of K_r catalyses the generative kind of chemical reaction causing an increment in the thickness of concentration boundary layer. Further, Fig. 26 infers that, with the progress of time species concentration is getting improved.

The change in behavior of primary as well as secondary shear stress components at the plate, under the influence of $m, M^2, K^2, K_1, G_r, G_c, N$ and ϕ derived from the expressions (25) and (26), are presented in Tables 1 and 2. One can observe from the tables that for both the kinds of thermal conditions at the plates, m, K_1, G_r, G_c lower the primary shear stress τ_x whilst an opposite nature is observed for M^2, K^2, N and ϕ. Again, from Tables 1 and 2 it is also revealed that, for both the kinds of thermal conditions at the plates, secondary shear stress τ_z becomes a growing function of m, M^2, K^2, K_1, G_r and G_c whereas the values of τ_z is getting lowered with the increment of N and ϕ.

Numerical calculations for heat transfer rate at the plate N_u, derived from Eqs. (27) and (28), have been presented in Table 3 for several values of N, ϕ and t. Table 3 shows that, for both the kinds of thermal conditions at the plates, N_u is getting enhanced with the growing values of either of N or ϕ. Furthermore, in case of ramped temperature plate, N_u gradually takes higher values with the advancement of time whereas a completely reverse phenomenon takes place when isothermal plate is considered.

The numerical values of mass transfer rate at the plate S_h, evaluated from Eq. (29) is shown in Table 4 under the influences of K_r and t. It is deduced from Table 4 that, S_h increases with the increment in the values of K_r whereas a reduction is noted with the progress of time t.

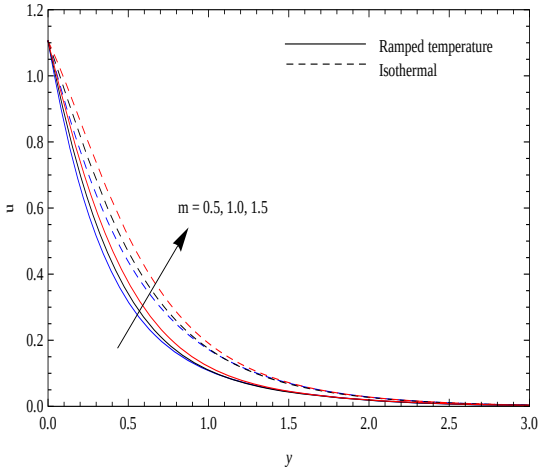

Fig. 2 Primary velocity profiles for m

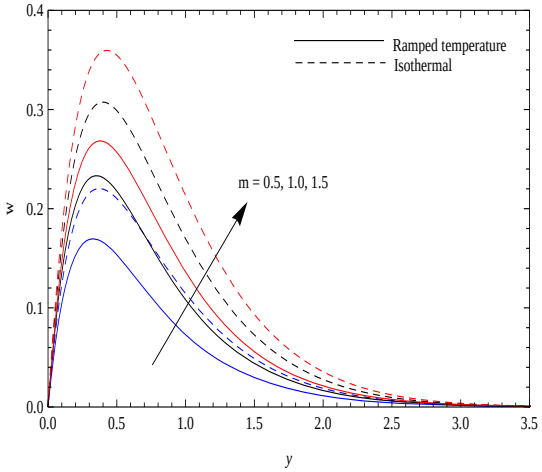

Fig. 3 Secondary velocity profiles for m

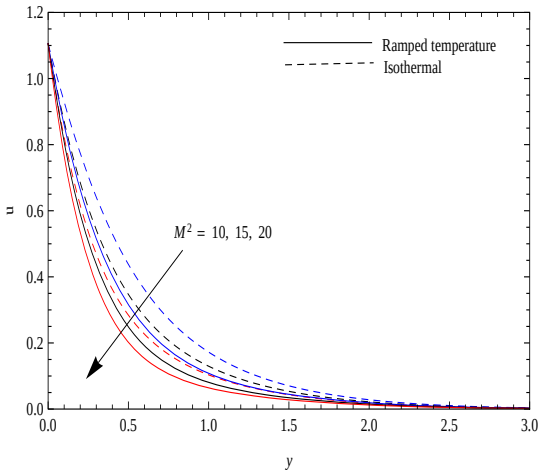

Fig. 4 Primary velocity profiles for M^2

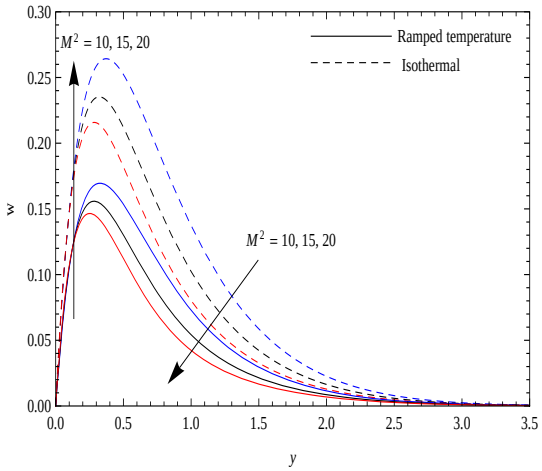

Fig. 5 Secondary velocity profiles for M^2

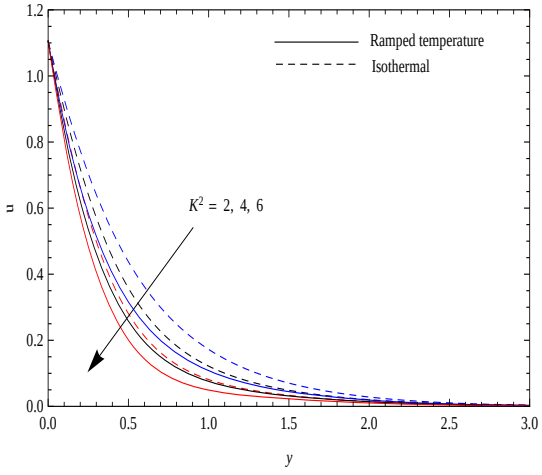

Fig. 6 Primary velocity profiles for K^2

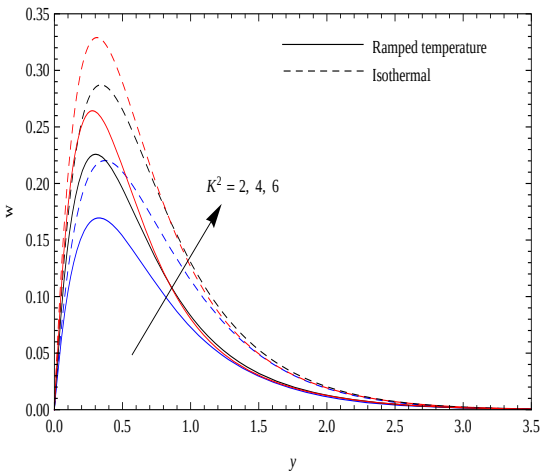

Fig. 7 Secondary velocity profiles for K^2

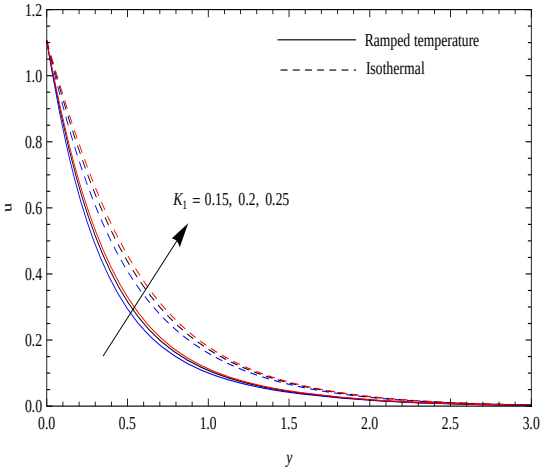

Fig. 8 Primary velocity profiles for K_1

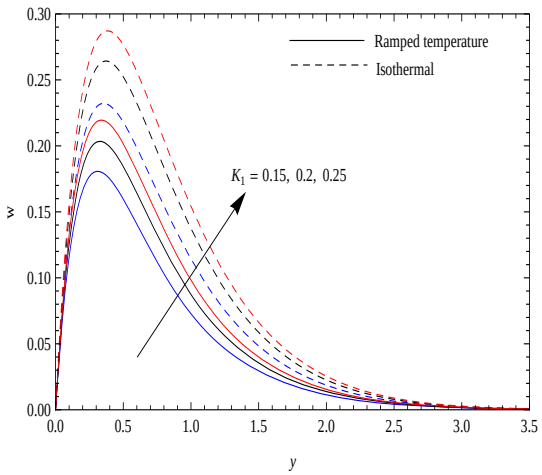

Fig. 9 Secondary velocity profiles for K_1

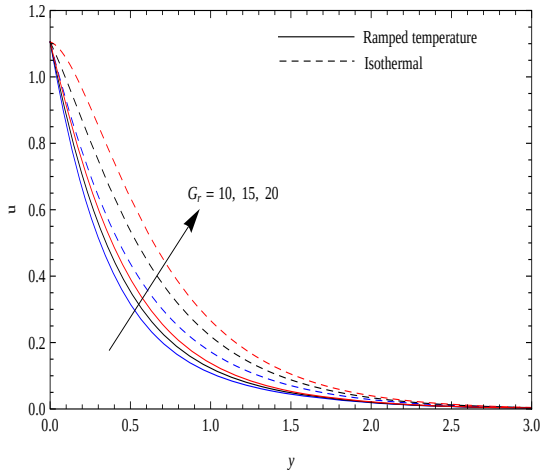

Fig. 10 Primary velocity profiles for G_r

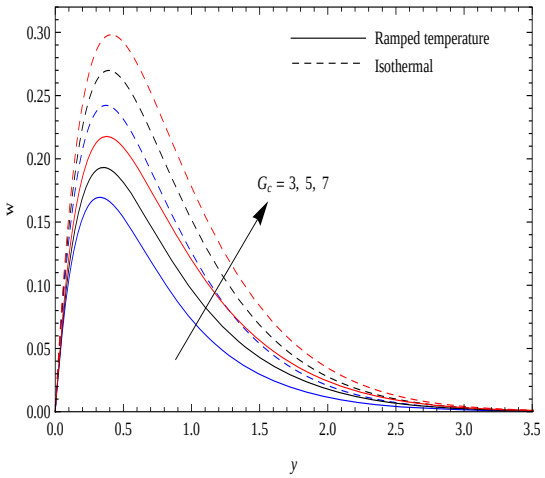

Fig. 13 Secondary velocity profiles for G_c

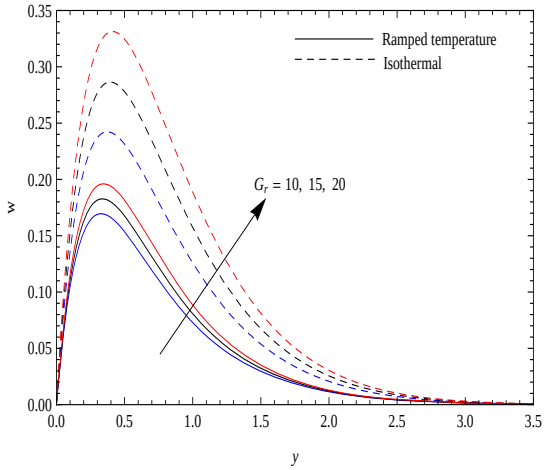

Fig. 11 Secondary velocity profiles for G_r

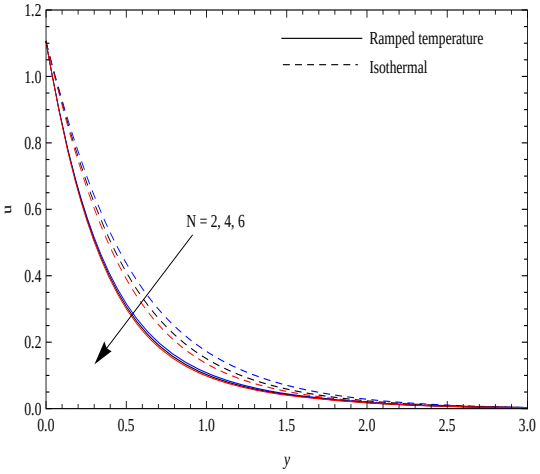

Fig. 14 Primary velocity profiles for N

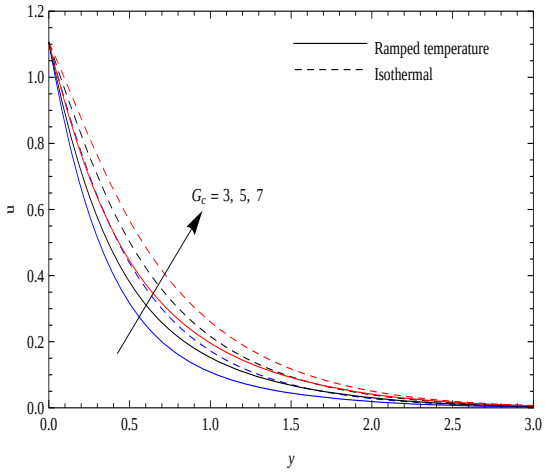

Fig. 12 Primary velocity profiles for G_c

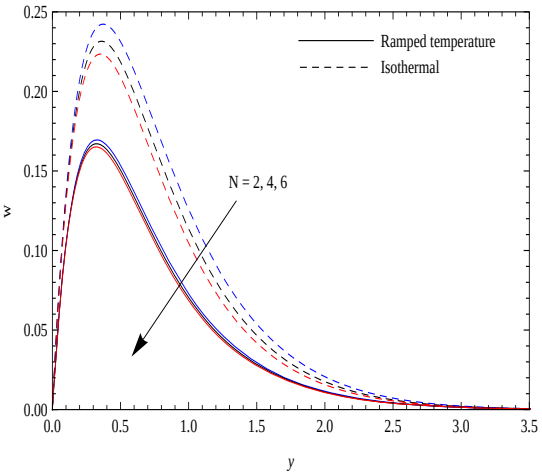

Fig. 15 Secondary velocity profiles for N

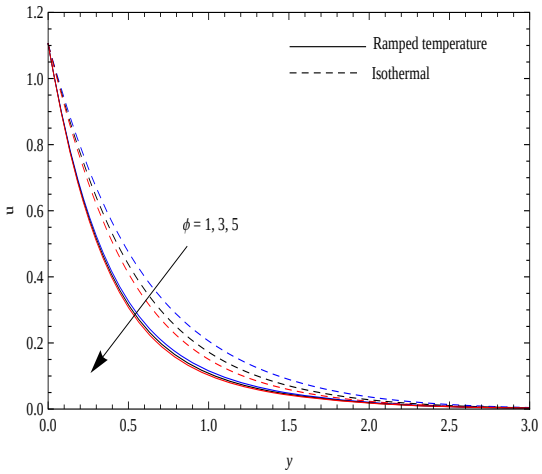

Fig. 16 Primary velocity profiles for ϕ

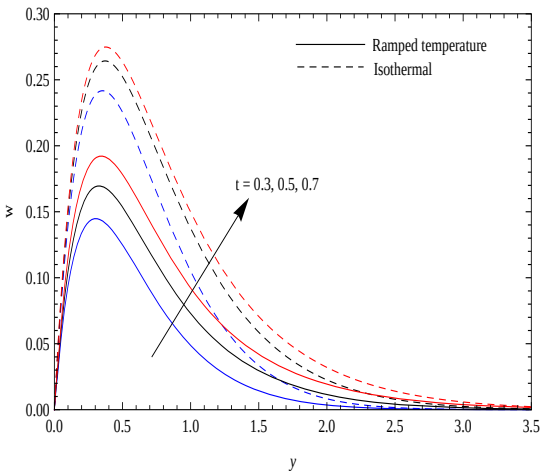

Fig. 19 Secondary velocity profiles for t

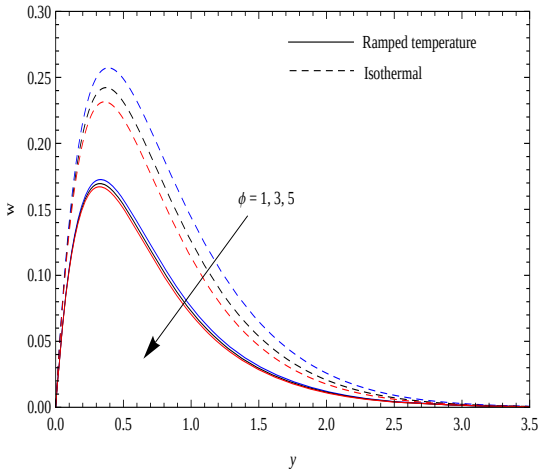

Fig. 17 Secondary velocity profiles for ϕ

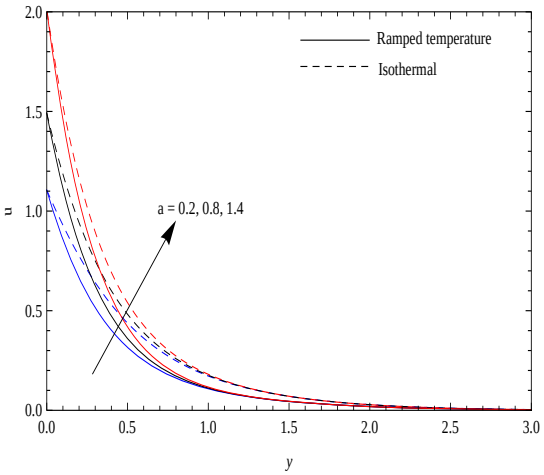

Fig. 20 Primary velocity profiles for a

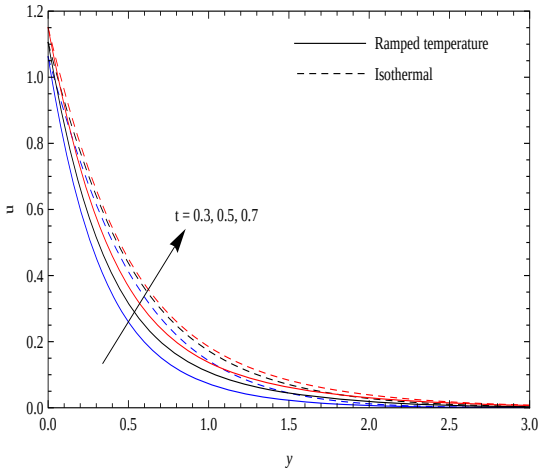

Fig. 18 Primary velocity profiles for t

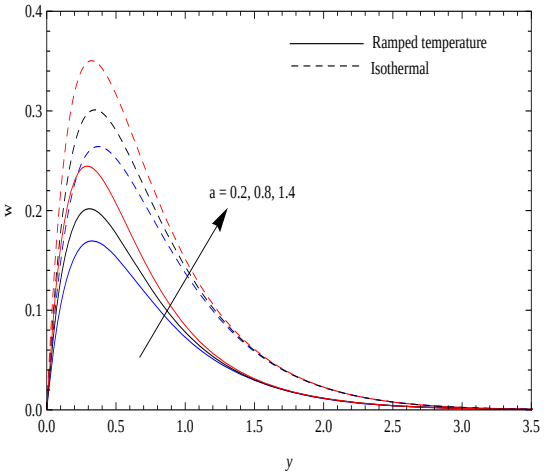

Fig. 21 Secondary velocity profiles for a

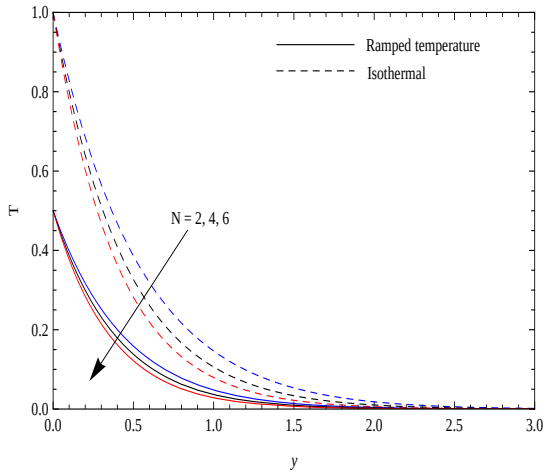

Fig. 22 Temperature profiles for N

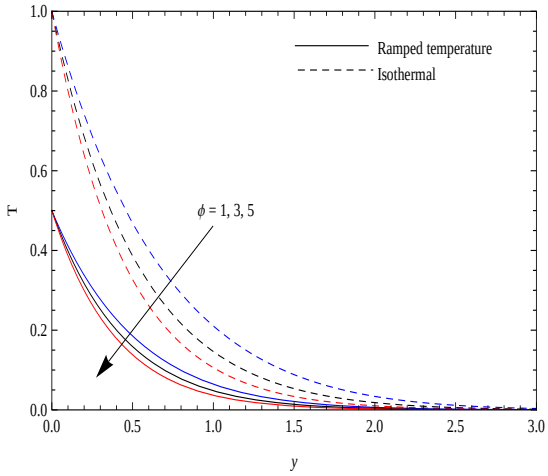

Fig. 23 Temperature profiles for ϕ

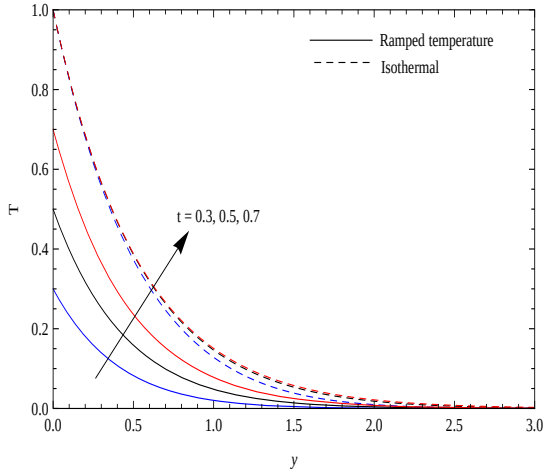

Fig. 24 Temperature profiles for t

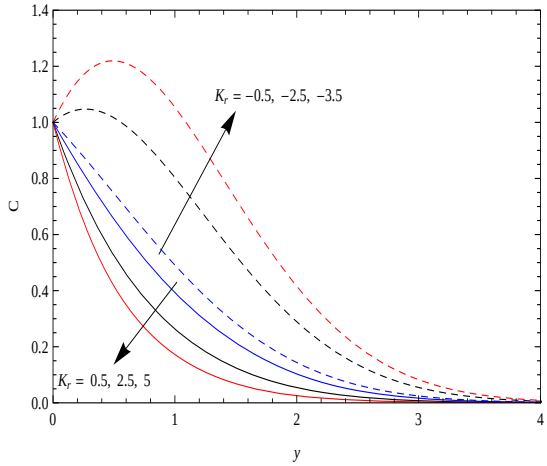

Fig. 25 Concentration profiles for K_r

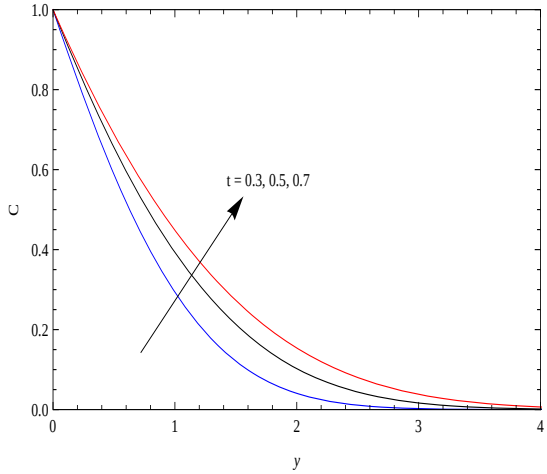

Fig. 26 Concentration profiles for t

Table 1 Shear stress at ramped temperature plate for different values of $m, M^2, K^2, K_1, G_r, G_c, N$ and ϕ.

m	M^2	K^2	K_1	G_r	G_c	N	ϕ	$-\tau_x$	τ_z
0.5								2.79124	1.42244
1.0	10	2	0.2	10	3	2	3	2.36605	1.78672
1.5								2.00415	1.88854
	10							2.79124	1.42244
0.5	**15**	2	0.2	10	3	2	3	3.48712	1.51988
	20							4.09237	1.61238
		2						2.79124	1.42244
0.5	10	**4**	0.2	10	3	2	3	3.04024	2.02350
		6						3.31976	2.54437
			0.15					3.05364	1.33680
0.5	10	2	**0.2**	10	3	2	3	2.79124	1.42244
			0.25					2.62812	1.48072
				10				2.79124	1.42244
0.5	10	2	0.2	**15**	3	2	3	2.40519	1.48133
				20				2.01914	1.54023
					3			2.79124	1.42244
0.5	10	2	0.2	10	**5**	2	3	2.37894	1.51329
					7			1.96664	1.60415
						2		2.79124	1.42244
0.5	10	2	0.2	10	3	**4**	3	2.82225	1.41352
						6		2.84858	1.40613
							1	2.75383	1.43345
0.5	10	2	0.2	10	3	2	**3**	2.79124	1.42244
							5	2.82225	1.41352

Table 2 Shear stress at isothermal plate for different values of $m, M^2, K^2, K_1, G_r, G_c, N$ and ϕ.

m	M^2	K^2	K_1	G_r	G_c	N	ϕ	$-\tau_x$	τ_z
0.5								1.85674	1.62212
1.0	10	2	0.2	10	3	2	3	1.39594	2.06245
1.5								0.98914	2.20835
	10							1.85674	1.62212
0.5	**15**	2	0.2	10	3	2	3	2.64142	1.69866
	20							3.31247	1.77632
		2						1.85674	1.62212
0.5	10	**4**	0.2	10	3	2	3	2.17136	2.28258
		6						2.51488	2.83873
			0.15					2.14892	1.51296
0.5	10	2	**0.2**	10	3	2	3	1.85674	1.62212
			0.25					1.67472	1.69700
				10				1.85674	1.62212
0.5	10	2	0.2	**15**	3	2	3	1.00344	1.78086
				20				0.15015	1.93960
					3			1.85674	1.62212
0.5	10	2	0.2	10	**5**	2	3	1.44444	1.71298
					7			1.03214	1.80383
						2		1.85674	1.62212
0.5	10	2	0.2	10	3	**4**	3	1.94575	1.59033
						6		2.01725	1.56559
							1	1.74116	1.66456
0.5	10	2	0.2	10	3	2	**3**	1.85674	1.62212
							5	1.94575	1.59033

Table 3 Variations in N_u for different values of N, ϕ and t

N	ϕ	t	ramped temperature plate $-N_u$	isothermal plate $-N_u$
2			1.12943	1.89157
4	3	0.5	1.27368	2.23148
6			1.40430	2.52849
	1		0.96696	1.48794
2	**3**	0.5	1.12943	1.89157
	5		1.27368	2.23148
		0.3	0.74900	1.92093
2	3	**0.5**	1.12943	1.89157
		0.7	1.50704	1.88595

Table 4 Variations in S_h for different values of K_r and t

K_r	t	$-S_h$
0.5		0.76642
2.5	0.5	1.26238
5.0		1.73888
	0.3	0.91466
0.5	**0.5**	0.76642
	0.7	0.69519

5. CONCLUSIONS

The noteworthy outcomes of the present study are as follows:

- For both ramped temperature and isothermal plates:
  - Hall effect, thermal and solutal buoyancy forces, permeability of the porous medium, time and surface acceleration parameter tend to enhance the primary fluid velocity whereas a reverse trend is followed by magnetic field, rotation, thermal radiation and heat absorption on the primary fluid flow all over the boundary layer region. The secondary velocity gets enhanced with the increment of Hall effect, permeability parameter, rotation, thermal and solutal buoyancy forces, time and surface acceleration parameter in the boundary layer region whereas an opposite pattern is noted for thermal radiation, magnetic parameter and heat absorption.
  - Heat absorption and thermal radiation tend to lower the temperature of the fluid whereas fluid temperature gets increased with the progress of time
  - Chemical reaction of destructive kind results in a decrement in the species concentration whereas a reverse tendency is followed in case of generative chemical reaction. Further, with the advancement of time, species concentration gets improved.
  - Primary shear stress component at the plate decreases as we increase Hall effect, solutal and thermal buoyancy forces and the permeability of the porous medium whereas an opposite trend is noticed for magnetic field, rotation, heat absorption, thermal radiation.
  - Secondary shear stress component at the plate gets enhanced on intensification of Hall effect, rotation, magnetic field, permeability of porous medium and thermal and solutal buoyancy forces whereas an adverse effect is observed for heat absorption and thermal radiation.
- Heat transfer rate at the plate gets improved as we amplify heat absorption and thermal radiation parameter for both the kinds of thermal conditions at the plates. Moreover, heat transfer rate in case of ramped temperature plate gets enhanced with the progress of time whereas an opposite trend is noticed for isothermal plate.
- Chemical reaction parameter increases the mass transfer rate at the plate whereas a contradictory pattern is noticed in case of time.

ACKNOWLEDGEMENTS

One of the authors Mr. Arnab Bhattacharyya is thankful to the Indian Institute of Technology (Indian School of Mines), Dhanbad, India for providing research fellowship to carry out this research work.

NOMENCLATURE

a	surface acceleration parameter
C'	species concentration (Kg)
c_p	specific heat at constant pressure (J/kg·K)
D_m	molecular mass diffusivity (m^2/s)
g	gravitational acceleration (m/s^2)
G_r	thermal Grashof number
G_c	solutal Grashof number
k	thermal conductivity of the fluid (W/m·K)
K^2	rotation parameter
K_r	chemical reaction parameter
K_1	permeability parameter
m	Hall current parameter
M^2	magnetic parameter
N	thermal radiation parameter

q_r' radiative heat flux (W/m^2)
Q_0 coefficient of heat absorption
t time (s)
T' fluid temperature (K)
u' velocity of the fluid along x' - axis (m/s)
w' velocity of the fluid along z' - axis (m/s)

Greek Symbols
β' coefficient of thermal expansion (K^{-1})
β^* coefficient of volumetric expansion (K^{-1})
ν kinematic coefficient of viscosity (m^2/s)
ρ density of the fluid (Kg/m^3)
σ electrical conductivity (S/m)
σ^* Stefan-Boltzmann constant (W/m^2 ·K^4)
τ_x primary shear stress at the plate (Kg/m.s^2)
τ_z secondary shear stress at the plate (Kg/m.s^2)
ϕ dimensionless heat absorption parameter

REFERENCES

Aboeldahab, E. M. and Elbarbary, E. M. E., 2001, "Hall Current Effect on Magnetohydrodynamic Free-Convection Flow Past a Semi-Infinite Vertical Plate with Mass Transfer," *International Journal of Engineering and Sciences*, **39**(14), 1641-1652.
https://dx.doi.org/10.1016/S0020-7225(01)00020-9

Afify, A. A., 2004, "Effect of Radiation on Free Convective Flow and Mass Transfer Past a Vertical Isothermal Cone Surface with Chemical Reaction in the Presence of a Transverse Magnetic Field," *Canadian Journal of Physics*, **82**(6), 447-458.
https://dx.doi.org/10.1139/p04-009

Bestman, A. R. and Adjepong, S. K., 1988, "Unsteady Hydromagnetic Free-Convection Flow with Radiative Heat Transfer in a Rotating Fluid," *Astrophysics and Space Science*, **143**(1), 73-80.
https://dx.doi.org/10.1007/BF00636756

Bhattacharyya, K. and Layek, G. C., 2012, "Similarity Solution of MHD Boundary Layer Flow with Diffusion and Chemical Reaction Over a Porous Flat Plate with Suction/Blowing," *Meccanica*, **47**(4), 1043-1048.
https://dx.doi.org/10.1007/s11012-011-9461-x

Chamkha, A. J., 2000, "Thermal Radiation and Buoyancy Effects on Hydromagnetic Flow Over an Accelerating Permeable Surface with Heat Source or Sink," *International Journal of Engineering and Science*, **38**(15), 1699-1712.
https://dx.doi.org/10.1016/S0020-7225(99)00134-2

Chamkha, A. J., 2003, "MHD Flow of a Uniformly Stretched Vertical Permeable Surface in the Presence of Heat Generation/Absorption and a Chemical Reaction," *International Communications in Heat and Mass Transfer*, **30**(3), 413-422.
https://dx.doi.org/10.1016/S0735-1933(03)00059-9

Chamkha, A. J., Mohamed, R. A. and Ahmed, S. E., 2011, "Unsteady MHD Natural Convection from a Heated Vertical Porous Plate in a Micropolar Fluid with Joule Heating, Chemical Reaction and Radiation Effects," *Meccanica*, **46**(2), 399-411.
https://dx.doi.org/10.1007/s11012-010-9321-0

Chandran, P., Sacheti, N. C. and Singh, A. K., 2005, "Natural Convection Near a Vertical Plate with Ramped Wall Temperature," *Heat and Mass Transfer*, **41**(5), 459-464.
https://dx.doi.org/10.1007/s00231-004-0568-7

Chen, C. H., 2004, "Combined Heat and Mass Transfer in MHD Free Convection from a Vertical Surface with Ohmic Heating and Viscous Dissipation," *International Journal of Engineering Science*, **42**(7), 699-713.
https://dx.doi.org/10.1016/j.ijengsci.2003.09.002

Cowling, T. G., 1957, *Magnetohydrodynamics*, Interscience Publishers, New York.

Cramer, R. and Pai, S. I., 1973, *Magnetofluid Dynamics for Engineers and Applied Physicists*, McGraw Hill Book Company, New York.

Das, S., Sarkar, B. C. and Jana, R. N., 2013, "Hall Effect on MHD Free Convection Boundary Layer Flow Past a Vertical Flat Plate," *Meccanica*, **48**(6), 1387-1398.
https://dx.doi.org/10.1007/s11012-012-9673-8

Hayat, T., Waqas, M., Ijaz Khan, M. and Alsaedi, A., 2017, "Impacts of Constructive and Destructive Chemical Reactions in Magnetohydrodynamic (MHD) Flow of Jeffrey Liquid due to Nonlinear Radially Stretched Surface," *Journal of Molecular Liquids*, **225**, 302-310.
https://dx.doi.org/10.1016/j.molliq.2016.11.023

Hayday, A. A., Bowlus, D. A. and McGraw, R. A., 1967, "Free Convection from a Vertical Flat Plate with Step Discontinuities in Surface Temperature," *Journal of Heat Transfer-ASME*, **89**(3), 244-249.
https://dx.doi.org/10.1115/1.3614371

Ibrahim, F. S., Elaiw, A. M. and Bakr, A., 2008, "Effect of the Chemical Reaction and Radiation Absorption on the Unsteady MHD Free Convection Flow Past a Semi-Infinite Vertical Permeable Moving Plate with Heat Source and Suction," *Communications in Nonlinear Science and Numerical Simulation*, **13**(6), 1056-1066.
https://dx.doi.org/10.1016/j.cnsns.2006.09.007

Kundu, P. K., Das, K. and Acharya, N., 2014, "Flow Features of a Conducting Fluid Near an Accelerated Vertical Plate in Porous Medium with Ramped Wall Temperature," *Journal of Mechanics*, **30**(3), 277-288.
https://dx.doi.org/10.1017/jmech.2014.14

Lee, S. and Yovanovich, M. M., 1991, "Laminar Natural Convection from a Vertical Plate with a Step Change in Wall Temperature," *Journal of Heat Transfer-ASME*, **113**(2), 501-504.
https://dx.doi.org/10.1115/1.2910591

Makinde, O. D., 2012, "Heat and Mass Transfer by MHD Mixed Convection Stagnation Point Flow Toward a Vertical Plate Embedded in a Highly Porous Medium with Radiation and Internal Heat Generation," *Meccanica*, **47**(5), 1173-1184.
https://dx.doi.org/10.1007/s11012-011-9502-5

Mbeledogu, I. U. and Ogulu, A., 2007, "Heat and Mass Transfer of an Unsteady MHD Natural Convection Flow of a Rotating Fluid Past a Vertical Porous Flat Plate in the Presence of Radiative Heat Transfer," *International Journal of Heat and Mass Transfer*, **50**(9-10), 1902-1908.
https://dx.doi.org/10.1016/j.ijheatmasstransfer.2006.10.016

Muthucumaraswamy, R., Chandrakala, P. and Raj, S. A., 2006, "Radiative Heat and Mass Transfer Effects on Moving Isothermal Vertical Plate in the Presence of Chemical Reaction," *International Journal of Applied Mechanics and Engineering*, **11**(3), 639-646.

Nagaraju, G., Matta, A. and Kaladhar, K., 2016, "Effects of Chemical Reaction and Thermal Radiation on Heat Generated Stretching Sheet in a Couple Stress Fluid Flow," *Frontiers in Heat and Mass Transfer*, **7**-11
https://dx.doi.org/10.5098/hmt.7.11

Pop, I. and Watanabe, T., 1994, "Hall Effects on Magnetohydrodynamic Free Convection about a Semi-Infinite Vertical Flat Plate," *International Journal of Engineering and Science*, **32**(12), 1903-1911.
https://dx.doi.org/10.1016/0020-7225(94)90087-6

Prasad, K. V., Datti, P. S. and Vajravelu, K., 2013, "MHD Mixed Convection Flow Over a Permeable Non-Isothermal Wedge," *Journal of King Saud University-Science*, **25**(4), 313-324.
https://dx.doi.org/10.1016/j.jksus.2013.02.005

Rajesh, V. and Chamkha, A. J., 2014, "Effects of Ramped Wall Temperature on Unsteady Two-Dimensional Flow Past a Vertical Plate with Thermal Radiation and Chemical Reaction," *Communications in Numerical Analysis*, **2014**(1), Article ID cna-00218.

Raptis, A. A. and Singh, A. K., 1985, "Rotation Effects on MHD Free-Convection Flow Past an Accelerated Vertical Plate," *Mechanics Research Communications*, **12**(1), 31-40.
https://dx.doi.org/10.1016/0093-6413(85)90032-1

Raptis, A., 2011, "Free Convective Oscillatory Flow and Mass Transfer Past a Porous Plate in the Presence of Radiation for an Optically Thin Fluid," *Thermal Science*, **15**(3), 849-857.
https://dx.doi.org/10.2298/TSCI101208032R

Reddy, M. G., 2014, "Influence of Thermal Radiation, Viscous Dissipation and Hall Current on MHD Convection Flow Over a Stretched Vertical Flat Plate," *Ain Shams Engineering Journal*, **5**(1), 169-175.
https://dx.doi.org/10.1016/j.asej.2013.08.003

Satya Narayana, P. V., Venkateswarlu, B. and Devika, B., 2016, "Chemical Reaction and Heat Source Effects on MHD Oscillatory Flow in an Irregular Channel," *Ain Shams Engineering Journal*, **7**(4), 1079-1088.
https://dx.doi.org/10.1016/j.asej.2015.07.012

Seth, G. S., Sarkar, S. and Mahato, G. K., 2013, "Effects of Hall Current on Hydromagnetic Free Convection Flow with Heat and Mass Transfer of a Heat Absorbing Fluid Past an Impulsively Moving Vertical Plate with Ramped Temperature," *International Journal of Heat and Technology*, **31**(1), 85-96.

Seth, G. S., Hussain, S. M. and Sarkar, S., 2014, "Effects of Hall Current and Rotation on Unsteady MHD Natural Convection Flow with Heat and Mass Transfer Past an Impulsively Moving Vertical Plate in the Presence of Radiation and Chemical Reaction," *Bulgarian Chemical Communications*, **46**(4), 704-718.

Seth, G. S., Sarkar, S., Hussain, S. M. and Mahato, G. K., 2015, "Effects of Hall Current and Rotation on Hydromagnetic Natural Convection Flow with Heat and Mass Transfer of a Heat Absorbing Fluid Past an Impulsively Moving Vertical Plate with Ramped Temperature ," *Journal of Applied Fluid Mechanics*, **8**(1), 159-171.

Seth, G. S. and Sarkar, S., 2015, "Hydromagnetic Natural Convection Flow with Induced Magnetic Field and nth Order Chemical Reaction of a Heat Absorbing Fluid Past an Impulsively Moving Vertical Plate with Ramped Temperature," *Bulgarian Chemical Communications*, **47**(1), 66-79.

Seth, G. S., Mandal, P. K. and Chamkha, A. J., 2016, "MHD Free Convective Flow Past an Impulsively Moving Vertical Plate with Ramped Heat Flux Through Porous Medium in the Presence of Inclined Magnetic Field," *Frontiers in Heat and Mass Transfer*, 7-23
https://dx.doi.org/10.5098/hmt.7.23

Singh, A. K., 1984, "MHD Free-Convection Flow Past an Accelerated Vertical Porous Plate in a Rotating Fluid," *Astrophysics and Space Science*, **103**(1), 155-163.
https://dx.doi.org/10.1007/BF00650053

Sreedevi, G, Raghavendra Rao, R., Prasada Rao, D. R. V. and Chamkha, A. J., 2016, "Combined Influence of Radiation Absorption and Hall Current Effects on MHD Double-Diffusive Free Convective Flow Past a Stretching Sheet," *Ain Shams Engineering Journal*, **7**(1), 383-397.
https://dx.doi.org/10.1016/j.asej.2015.11.024

Sutton, G. W. and Sherman, A., 1965, *Engineering Magnetohydrodynamics*, New York: McGraw-Hill.

Veeresh, C., Varma, S. V. K., Vijaya Kumar, A. G., Umamaheswar, M. and Raju, M. C., 2017, "Joule Heating and Thermal Diffusion Effects on MHD Radiative and Convective Casson Fluid Flow Past an Oscillating Semi-Infinite Vertical Porous Plate," *Frontiers in Heat and Mass Transfer*, 8-1
https://dx.doi.org/10.5098/hmt.8.1

APPENDIX

$$g_1(d_1,d_2,d_3,d_4,d_5)=\frac{1}{2}[e^{d_1\sqrt{d_3(d_4+d_5)}}erfc\left(\frac{d_1}{2}\sqrt{\frac{d_3}{d_2}}+\sqrt{d_2(d_4+d_5)}\right)+$$
$$e^{-d_1\sqrt{d_3(d_4+d_5)}}erfc\left(\frac{d_1}{2}\sqrt{\frac{d_3}{d_2}}-\sqrt{d_2(d_4+d_5)}\right)]$$

$$g_2(d_1,d_2,d_3,d_4)=\frac{1}{2}\left(d_2+\frac{d_1}{2}\sqrt{\frac{d_3}{d_4}}\right)e^{c_1\sqrt{d_3d_4}}erfc\left(\frac{d_1}{2}\sqrt{\frac{d_3}{d_2}}+\sqrt{d_2d_4}\right)+$$
$$\frac{1}{2}\left(d_2-\frac{d_1}{2}\sqrt{\frac{d_3}{d_4}}\right)e^{-d_1\sqrt{d_3d_4}}erfc\left(\frac{d_1}{2}\sqrt{\frac{d_3}{d_2}}-\sqrt{d_2d_4}\right)$$

$$g_3(d_1,d_2,d_3,d_4)=\sqrt{d_2(d_3+d_4)}\left\{erfc\left(\sqrt{d_1(d_3+d_4)}\right)-1\right\}-$$
$$e^{-d_1(d_3+d_4)}\sqrt{\frac{d_2}{\pi d_1}}$$

$$g_4(d_1,d_2,d_3)=\frac{1}{2}[\left(\sqrt{\frac{d_2}{d_3}}+2d_1\sqrt{d_2d_3}\right)\left\{erfc\left(\sqrt{d_1d_3}\right)-1\right\}-$$
$$2e^{-d_1d_3}\sqrt{\frac{d_1d_2}{\pi}}]$$